

CCR: Facial Image Editing with Continuity, Consistency and Reversibility

Nan Yang, Xin Luan, Huidi Jia, Zhi Han *Member, IEEE*, and Yandong Tang* *Member, IEEE*

Abstract—Three problems exist in sequential facial image editing: incontinuous editing, inconsistent editing, and irreversible editing. Incontinuous editing is that the current editing can not retain the previously edited attributes. Inconsistent editing is that swapping the attribute editing orders can not yield the same results. Irreversible editing means that operating on a facial image is irreversible, especially in sequential facial image editing. In this work, we put forward three concepts and corresponding definitions: editing continuity, consistency, and reversibility. Then, we propose a novel model to achieve the goal of editing continuity, consistency, and reversibility. A sufficient criterion is defined to determine whether a model is continuous, consistent, and reversible. Extensive qualitative and quantitative experimental results validate our proposed model, and show that a continuous, consistent and reversible editing model has a more flexible editing function while preserving facial identity. Furthermore, we think that our proposed definitions and model will have wide and promising applications in multimedia processing. Code and data are available at <https://github.com/mickoluan/CCR>.

Index Terms—facial image editing, continuity, consistency, reversibility.

I. INTRODUCTION

FACIAL image editing has attracted extensive attention with the development of adversarial neural networks [1]–[5]. AttGAN [6] adopts reconstruction learning, adversarial learning, and an attribute classification constraint to achieve facial image editing. STGAN [7] enhances the editing performance of AttGAN by incorporating encoder-decoder and selective transfer units. ELEGANT [8] encodes different attributes into disentangled parts and generates images with other attributes by swapping certain parts of latent encodings. Liu et al. organize attribute labels into a hierarchical tree structure and propose a Hierarchical Style Disentanglement (HiSD) [9] method for facial image editing. Other works [10]–[15] achieve facial image editing based on a style-based architecture [16]–[18] and some explicable semantics [19]–[23].

These facial image editing methods mentioned above and other works [24], [25] have three common problems: incontinuous editing, inconsistent editing, and irreversible editing. An incontinuous and inconsistent editing case is shown in Fig. 1(a). We observe that: 1) the current editing can not retain the previously edited attributes, e.g., glasses; and 2) the both

N. Yang, X. Luan, B. J. Xia, H. D. Jia, Z. Han, and Y. D. Tang are with State Key Laboratory of Robotics, Shenyang Institute of Automation, Chinese Academy of Sciences, Shenyang 110016, China, and also Institutes for Robotics and Intelligent Manufacturing, and also University of Chinese Academy of Sciences, Beijing 100049, China (e-mail: yangnan@sia.cn; luanxin@sia.cn; jiahuidi@sia.cn; hanzhi@sia.cn; ytang@sia.cn). * Corresponding author.

final editing results are inconsistent when swapping attribute editing orders. Another editing case is shown in Fig. 1(b), and we can see that the editing process is irreversible. The reason is that existing methods do not consider whether a model is continuous, consistent, and reversible.

These three problems motivate us to study a novel model, which fully considers editing continuity, consistency, and reversibility. The model should ensure that 1) the current editing can retain the previously edited attributes while preserving facial identity; 2) it can yield a consistent editing result even though swapping attribute editing orders; and 3) a facial image editing is reversible. For these purposes, we propose a continuous, consistent and reversible model to achieve the goal of editing continuity, consistency, and reversibility. The editing results of proposed model are shown in Fig. 2, and we can 1) re-edit an edited face with other attributes sequentially; 2) get a consistent editing result despite swapping attribute editing orders; and 3) obtain a reversible editing result. The results indicate that our novel model can overcome the three problems existing in current methods.

Extensive experimental results show that our proposed model achieves the goal of editing continuity, consistency, and reversibility. It also can be used to analyse disentangled attributes and the trade-off between image editing and reconstruction. We further investigate a criterion, which can be used to determine whether the model is satisfied with continuity, consistency, and reversibility. Our unique contribution that advances the field of facial image editing contains three aspects:

1) We define three concepts for facial image editing, i.e., continuity, consistency, and reversibility. Then, we propose a novel model named CCR to achieve the desired goal;

2) We propose a progressive training strategy to train CCR, and then propose a criterion that can be used to determine whether a model is continuous, consistent, and reversible;

3) We draw an important conclusion that the necessary conditions for editing continuity, consistency, and reversibility are: a generalized encoder, disentangled style codes, and accurate attention regions.

II. PROPOSED METHOD

In this section, we 1) describe the label structure and editing path; 2) present the framework of CCR model; 3) exhibit its training objective; 4) give a criterion to evaluate CCR model.

A. Preliminary

We denote a facial image x that has the attribute j for the domain i as x_i^j . In addition, x_i^j has its style s_i^j . Assuming

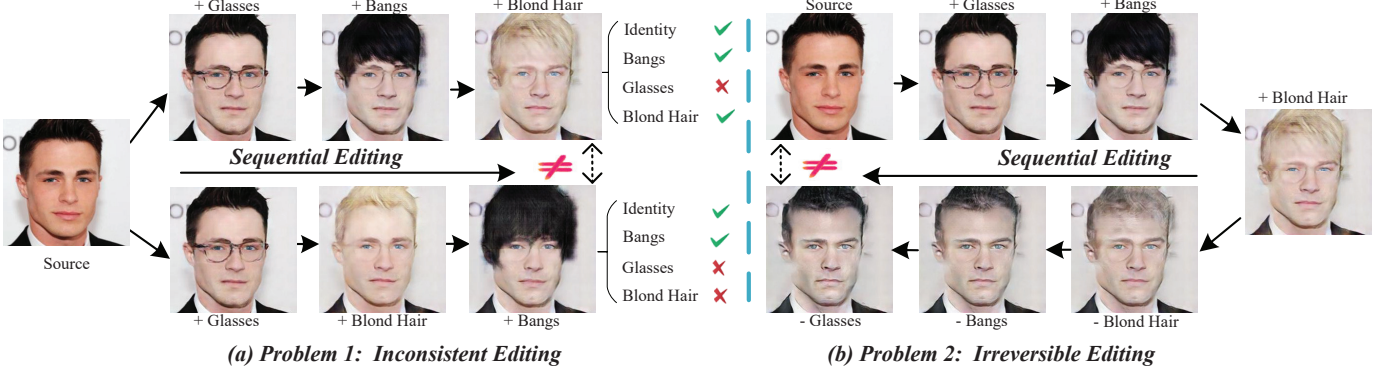


Fig. 1. A case of inconsistent and irreversible editing.

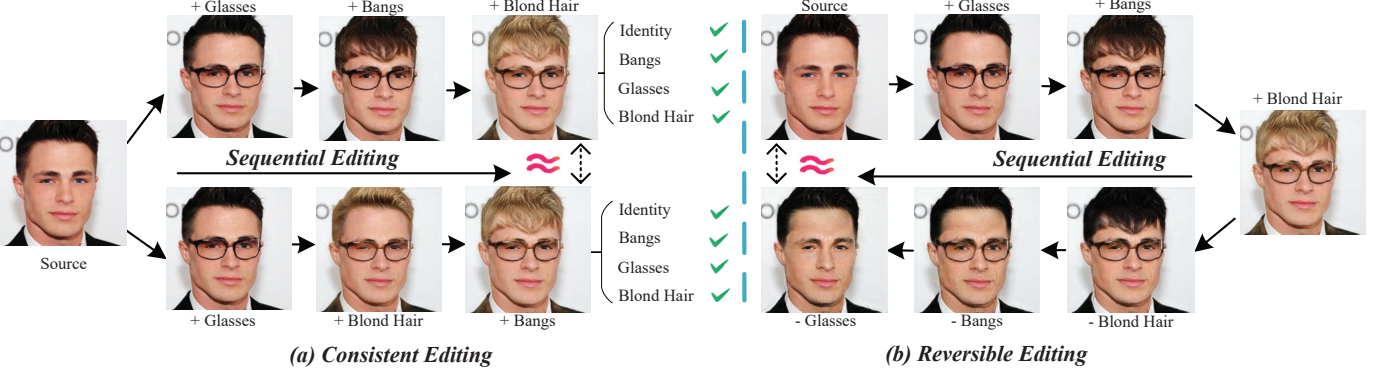


Fig. 2. A case of editing continuity, consistency, and reversibility, which is obtained using our proposed model (CCR).

that the editing path is from hair color domain to bangs domain and then to glasses domain, we sample a facial image randomly, male/female with black hair, without bangs, and without glasses. To present a clear editing path, we use a fixed attribute editing order, as shown in Fig. 4. Note that we can train CCR model in an arbitrary editing path. One editing path is:

$$x_0^0 \rightarrow x_0^1 \rightarrow x_1^1 \rightarrow x_2^1 \quad (1)$$

x_2^1 in Eq. (1) should be with blond hair, bangs, and glasses. This is our defined concept of editing continuity. Another editing path is:

$$x_0^0 \rightarrow x_0^1 \rightarrow x_2^1 \rightarrow x_1^1 \quad (2)$$

x_1^1 in Eq. (2) should be consistent with x_2^1 in Eq. (1) even though swapping attribute editing orders. This is our defined concept of editing consistency. The reversible editing path is defined as:

$$x_0'^0 \leftarrow x_0'^1 \leftarrow x_1'^1 \leftarrow x_2^1 \quad (3)$$

$x_0'^0$ should be a face with black hair, without bangs, and without glasses, and $x_0'^0$ should be equal to x_0^0 .

B. Framework

The framework of CCR model is shown in Fig. 3. We should train CCR model that can edit a facial image in a specific domain firstly, e.g., from black hair to blond hair in the domain of hair color in Fig. 3(a). The encoder E aims to encode a facial image to a latent code $z = E(x_0^0)$. z contains

hair color and facial identity information, etc. The CNN blocks learn to generate hair color styles s from a normal distribution [26]. z and s have the same dimension. We introduce an attention module M [27], [28] and an affine transformation T to focus on specific regions and disentangles hair color styles respectively, i.e., $m = M(s)$, $t = T(s)$. Then, we fuse m , z , and t using $\sigma(m) \cdot z + (1 - \sigma(m)) \cdot t$, where $\sigma(\cdot)$ is the sigmoid function, and $\sigma(m)$ is an attention mask. As noted in [9], this design can avoid global manipulations like background and illumination during translations with little additional calculation and no regularization objective. Finally, the fused feature is fed to G and generated an edited facial image x_0^1 with blond hair. L_1 is a loss function [29], [30] to measure the spatial distance between x_0^0 and $x_0'^0$.

Fig. 3(b) illustrates the editing pipeline from blond hair to black hair. Different from forward editing process, CCR receives source facial image x_0^0 and edited image x_0^1 as inputs. The CNN blocks in the backward module extract hair color styles from source facial image. We expect to return a facial image $x_0'^0$ with black hair that is equal to x_0^0 . We simplify the forward module and the backward module as FM and BM . Fig. 3(c) exhibits a case of consistent editing in multi-domain. Its corresponding editing path is Eqs. (1) and (2). Fig. 3(d) describes the case of reversible editing in multi-domain. Its corresponding editing is Eqs. (1) and (3). We can easily observe that editing continuity is an essential premise to achieve the goal of editing consistency and reversibility.

Training strategy. Note that the translated modules (FM

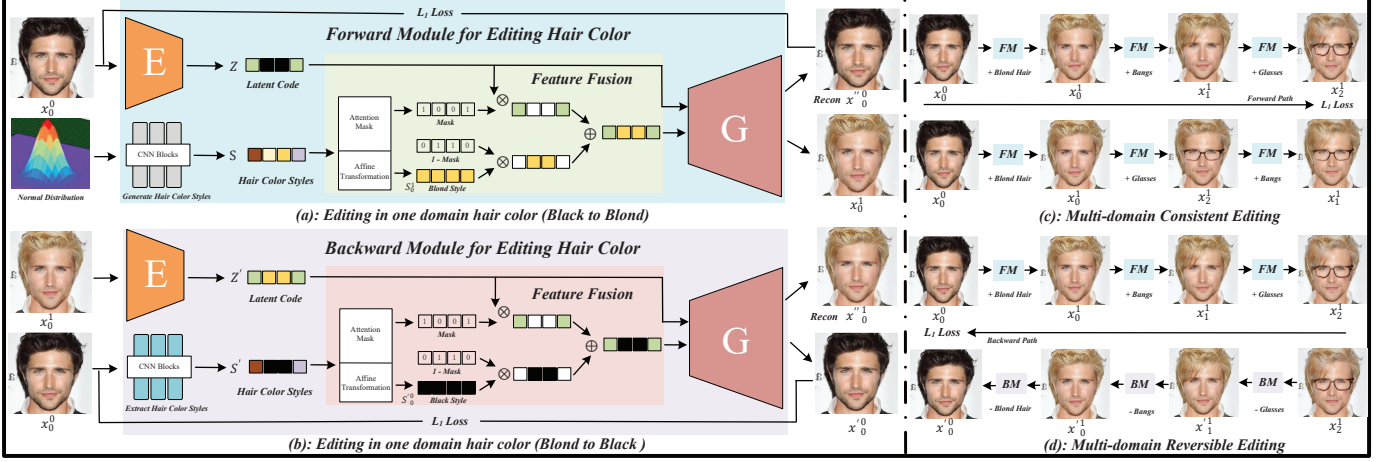


Fig. 3. The training pipeline of our method, which includes: a) Forward Module for editing in one domain; b) Backward Module for editing in one domain; c) Multi-domain Consistent Editing; d) Multi-domain Reversible Editing. Notice that the discriminator D is not shown but is used for training.

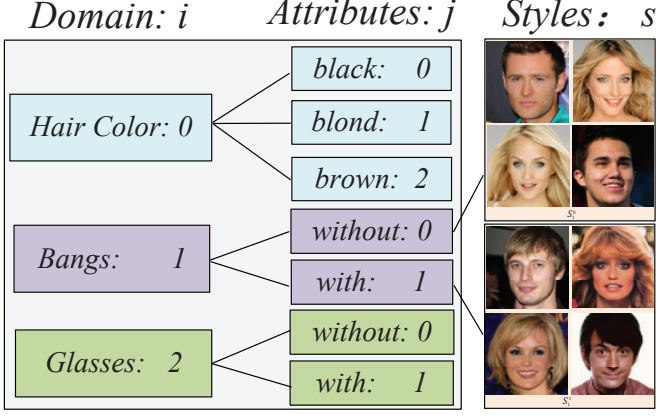


Fig. 4. The introduced hierarchical tree structure [9] with multi-domain and various attributes.

and BM) for a different domain are independent while the encoder (E) and generator (G) are shared and general. The shared part is regarded as an interface that matches multiple domains or categories. We use a progressive way to train our model. It contains three parts: 1) using an end-to-end strategy to train the shared encoder and generator. 2) using a one-to-one strategy to train different domains translated modules based on the well-trained shared parts. We can obtain independent translated modules for different domains. 3) selecting arbitrary editing paths and finetuning all the well-trained modules. Only updating the parameters of selected translated modules while freezing the parameters of shared and other translated modules in each iteration. Therefore, we can select and test any translated modules independently for translation to realize sequential editing.

C. Optimization objective

Adversarial loss. The model should treat all the generated facial images as fakes [31]–[33], except for the source image. The discriminator D is used to evaluate whether a facial image

is real or not. The adversarial objective is defined as:

$$\begin{aligned} \mathcal{L}_{adv} = & \mathbb{E} [\log (D (x_0^0))] + \mathbb{E} [\log (D (1 - x_0^1))] \\ & + \mathbb{E} [\log (D (1 - x_1^1))] + \mathbb{E} [\log (D (1 - x_2^1))] \\ & + \mathbb{E} [\log (D (1 - x_1'^1))] + \mathbb{E} [\log (D (1 - x_0'^1))] \\ & + \mathbb{E} [\log (D (1 - x_0'^0))] \end{aligned} \quad (4)$$

where, x_0^0 is a source facial image. x_0^1 , x_1^1 and x_2^1 are the translated images using FM , while $x_1'^1$, $x_0'^1$ and $x_0'^0$ are the reversed facial images using BM . \mathcal{L}_{adv} encourages the generator G to yield a high-quality facial image to support editing continuity.

Reconstruction loss. The model should reconstruct source image x_0^0 in the forward editing process. To achieve editing continuity, the model should also reconstruct an edited facial image x_0^1 in the backward editing process. Thus, we introduce a reconstructive objective [34] to force CCR to reduce the difference between source image and its corresponding edited one. We have the following reconstruction loss:

$$\begin{aligned} \mathcal{L}_{rec} = & \mathbb{E} [\|x_0^0 - x_0'^0\|_1] + \mathbb{E} [\|x_0^1 - x_0'^1\|_1] \\ & + \mathbb{E} [\|x_1^1 - x_1'^1\|_1] + \mathbb{E} [\|x_2^1 - x_2'^1\|_1] \end{aligned} \quad (5)$$

\mathcal{L}_{rec} : 1) encourages E to retain global facial features; 2) promotes G to generate a facial image that is equal to the source one; and 3) forces CNN blocks to extract attribute styles from a given facial image accurately.

Consistency loss. To retain editing consistency, we introduce the following consistency loss:

$$\mathcal{L}_{con} = \mathbb{E} [\|x_1^1 - x_2^1\|_1] \quad (6)$$

\mathcal{L}_{con} aims to reduce the difference between x_1^1 and x_2^1 . The two editing results are expected to have the same attributes and facial identity.

Reversibility loss. To achieve editing reversibility, we introduce the following reversibility loss:

$$\begin{aligned} \mathcal{L}_{rev} = & \mathbb{E} [\|x_1^1 - x_1'^1\|_1] \\ & + \mathbb{E} [\|x_0^1 - x_0'^1\|_1] + \mathbb{E} [\|x_0^0 - x_0'^0\|_1] \end{aligned} \quad (7)$$

\mathcal{L}_{rev} encourages the model to return a facial image that is equal to the source one at every stage.

Style loss. The extracted style codes for the edited facial image in BM should be equal to the generated style code from FM [31], [35]–[37]. We denote the function of extract style codes as $F(\cdot)$, then we have the following style loss:

$$\mathcal{L}_{sty} = \mathbb{E} [\|F(x_0^1) - s_0^1\|_1] + \mathbb{E} [\|F(x_1^1) - s_1^1\|_1] + \mathbb{E} [\|F(x_2^1) - s_2^1\|_1] \quad (8)$$

\mathcal{L}_{sty} keeps the consistency between the generated and extracted styles. The objective is to ensure that we can return a facial image with the same attributes.

Overall loss. We optimize the model in an editing path within the following objective:

$$\min_{E,G,F} \max_D \mathcal{L}_{adv} + \lambda_{rec} \mathcal{L}_{rec} + \lambda_{con} \mathcal{L}_{con} + \lambda_{rev} \mathcal{L}_{rev} + \lambda_{sty} \mathcal{L}_{sty} \quad (9)$$

where λ_{rec} , λ_{con} , λ_{rev} and λ_{sty} are positive hyper-parameters that control reconstruction, consistency, reversibility, and style objectives. The full objective guarantees CCR is a continuous, consistent, and reversible model.

D. Criterion

To evaluate continuity and consistency, we must judge all the attributes are added to the final desired editing facial image. For this purpose, we define the editing accuracy in multi-domain as:

$$EAC = \frac{\sum_1^m \sum_i^n H(\text{cls}(x_i), y_i)}{m * n} \quad (10)$$

where, m denotes the number of edited facial images and n indicates the number of domains. x_i denotes an edited facial image in domain i , while y_i denotes its corresponding true label. cls is a well-trained classifier, which outputs the predicted binary label for a facial image. H denotes Hamming distance [38], which computes the number of different bits in binary. EAC computes the sum of editing accuracy for each domain.

To evaluate reversibility, we need to determine if all the edited attributes are removed from the final editing facial image, i.e., remove accuracy:

$$RAC = 1 - \frac{\sum_1^m \sum_i^n H(\text{cls}(x'_i), y_i)}{m * n} \quad (11)$$

where x'_i denotes a reversed facial image in domain i .

Evaluating a model with EAC and RAC only from attribute level is not sufficient. We further assess the edited facial image quantificationally by using multi-scale metrics, e.g., MSE [39], RMSE [40], PSNR [41], UQI [42], SSIM [43], MS-SSIM [44], VSI [45], VIF [46], FSIM [47], GMSD [48], LPIPS [49], DISTs [50]. The model has higher values in all the above metrics, and the better it is. We evaluate CCR from both attribute and image levels, and the results are more reliable than that with a single metric.

III. EXPERIMENTAL RESULTS AND ANALYSIS

In this section, we 1) describe the experimental implementation details; 2) present single attribute editing results; 3) show

the editing results of continuity and consistency; 4) illustrate the editing results of reversibility; and 5) provide the results of ablation studies.

A. Implementation details

We train CCR model on the CelebA-HQ [51] dataset, which contains 30000 facial images with label annotations [52]. Five attributes are chosen in three domains, i.e., hair color, bangs, glasses. We divide the datasets into training and testing sets containing 27000 and 3000 images, respectively. Our experimental environment is based on Lenovo Intelligent Computing Orchestration (LiCO), a software solution that simplifies the use of clustered computing resources for artificial intelligence (AI) model development and training. All experiments are conducted in PyTorch 1.7 [53], CUDA 10.2, and CUDNN 10.2 with 8 NVidia Tesla V100 (32G) dual-channel graphics processing units (GPUs).

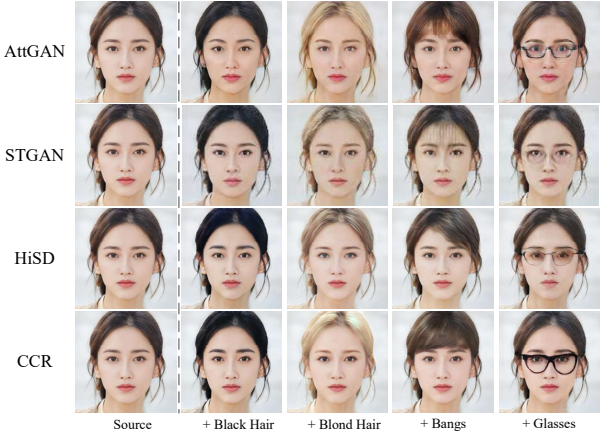


Fig. 5. The compared editing results with AttGAN [6], STGAN [7], HiSD [9] in one domain.

B. Single Attribute Editing

We evaluate the performance of CCR in one domain and compare it with three competing methods, i.e., AttGAN [6], STGAN [7], and HiSD [9]. AttGAN and STGAN are designed for facial image editing. HiSD is the current challenging facial image editing method. The qualitative results are shown in Fig. 5. We have three observations: 1) AttGAN and STGAN are still limited to editing glasses; 2) AttGAN attempts to change the color of bangs while STGAN has bangs that are not obvious; 3) HiSD yields a good editing result compared to AttGAN and STGAN. Unfortunately, the hair is not edited to blond completely. In comparison, CCR can edit the desired attributes effectively and correctly and yield results with high image quality.

The proposed CCR can extract style codes from different reference images. These codes can be used to perform custom facial image editing. The qualitative results in comparison to HiSD are shown in Fig. 6. We can observe: 1) both methods can extract diverse codes from reference images and add corresponding styles to source facial images, i.e., bangs and glasses; 2) the styles of bangs extracted using HiSD

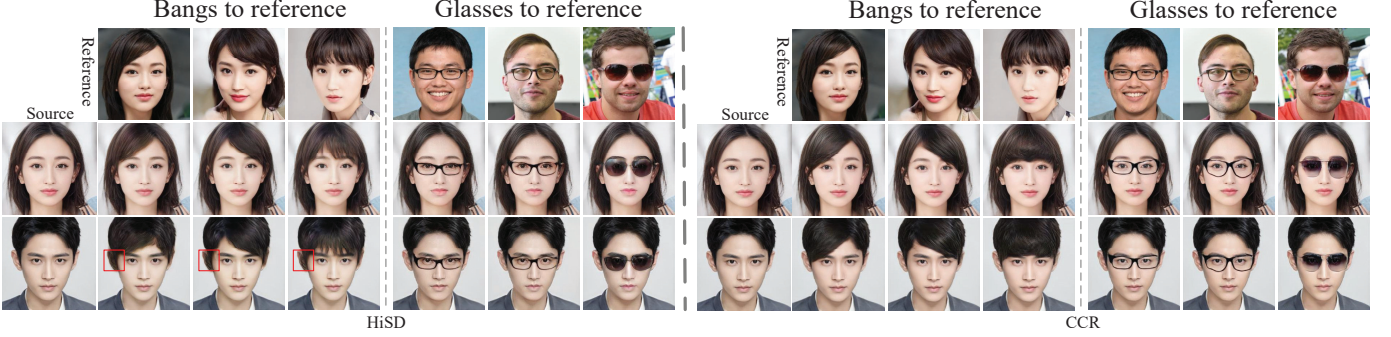


Fig. 6. The compared editing results with HiSD [9], where the styles are extracted from the reference facial images. Image artifacts are labeled with a red box in poorly edited images.

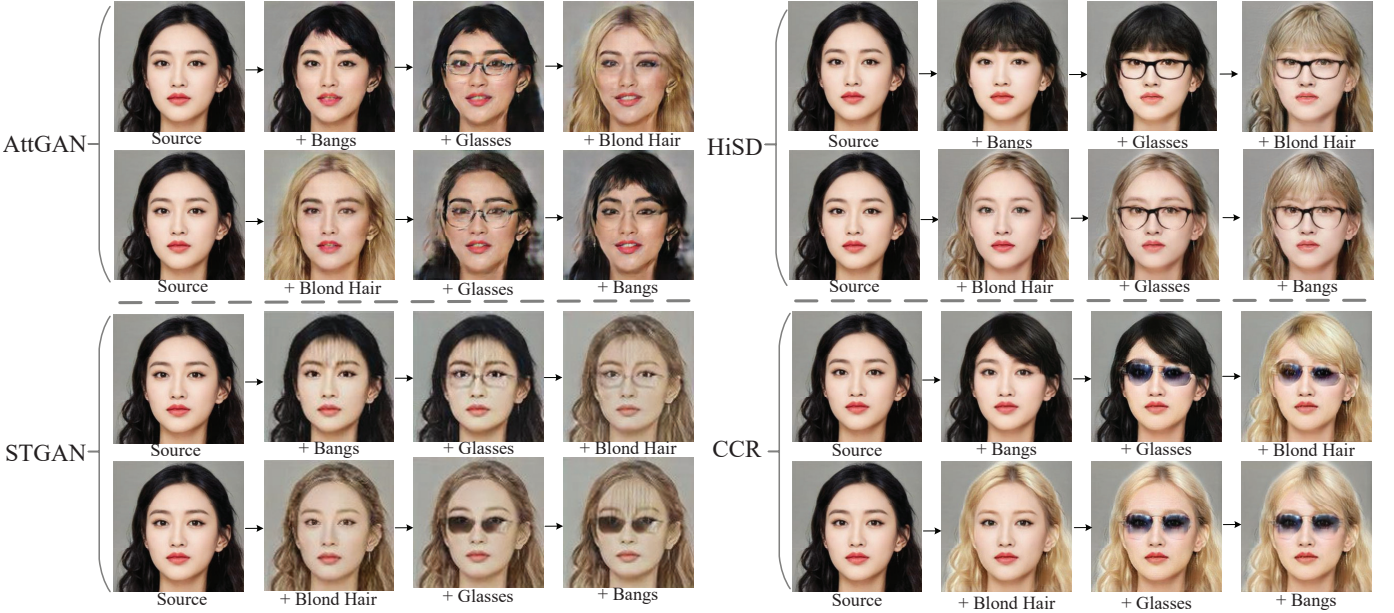


Fig. 7. The editing result of the editing continuity and consistency compared to AttGAN [6], STGAN [7], HiSD [9].

TABLE I
THE COMPARED SINGLE EAC WITH ATTGAN [6], STGAN [7], HiSD [9]
IN ONE DOMAIN.

Configuration	Bangs	Black Hair	Blond Hair	Brown Hair	Glasses
AttGAN [6]	0.8640	0.9237	0.7225	0.5354	0.9437
STGAN [7]	0.7113	0.8274	0.4158	0.5229	0.9111
HiSD [9]	0.7406	0.8669	0.6864	0.5768	0.7769
CCR	0.9066	0.8935	0.8064	0.6100	0.9265

are maybe over reliant their reference images. This reliance sometimes results in image artifacts, as shown in the red box in Fig. 6. CCR uses reconstruction loss in multi-domain and will not yield such cases. The experimental results show that CCR can extract style codes from reference images accurately and perform custom facial image editing well.

We evaluate the attribute editing accuracy quantitatively by re-using a pre-trained classification model, which can attain an accuracy of 94.5% on the test set [7]. The experimental results are shown in Table I. CCR outperforms HiSD on all the attributes. Besides, it exceeds the professional editing methods of AttGAN and STGAN on most of attributes, e.g.,

bangs, blond and brown hair. We are slightly less accurate than AttGAN in editing glasses. However, we observe that AttGAN has a poor image quality, which results in a woman who do not wear glasses being misjudged as wearing glasses, as shown in Fig. 5. CCR can also add diverse glasses styles to a person in comparison to AttGAN and STGAN.

C. Continuity and Consistency

As noted in Sec. II-B, editing continuity is an essential premise to consistency. Thus, we present these two concepts into one subsection. The qualitative results in comparison to three competing methods are shown in Fig. 7.

Editing continuity: AttGAN and STGAN can not retain the edited attributes. The image quality deteriorates, and facial identity is lost in performing editing sequentially. The results illustrate that both methods do not have the property of editing continuity. HiSD can retain the edited attributes while preserving facial identity. However, the blond hair is disturbed by black hair and not edited successfully. CCR can retain the edited attributes and preserve facial identity well. Furthermore, the blond is edited completely and not disturbed by black

TABLE II

THE QUANTITATIVE RESULTS OF EVALUATING EDITING CONTINUITY AND CONSISTENCY USING EAC AND IMAGE QUALITY METRICS. \uparrow AND \downarrow DENOTE THE HIGHER AND THE LOWER THE BETTER, RESPECTIVELY. METHODS WITH THE BEST AND RUNNER-UP PERFORMANCES ARE COLORED WITH RED AND BLUE, RESPECTIVELY

Method	EAC \uparrow		MSE \downarrow	RMSE \downarrow	UQI \uparrow	SSIM \uparrow	PSNR \uparrow	MS-SSIM \uparrow
	Path 1	Path 2						
AttGAN [6]	36.46%	31.15%	0.0272	0.1569	0.8771	0.8261	16.5303	0.8330
STGAN [7]	40.24%	47.53%	0.0115	0.1003	0.8610	0.8788	20.5773	0.9109
HiSD [9]	52.99%	57.19%	0.0107	0.0997	0.9023	0.8625	20.3696	0.8989
CCR	59.41%	60.49%	0.0096	0.0943	0.9173	0.8847	20.8347	0.9196

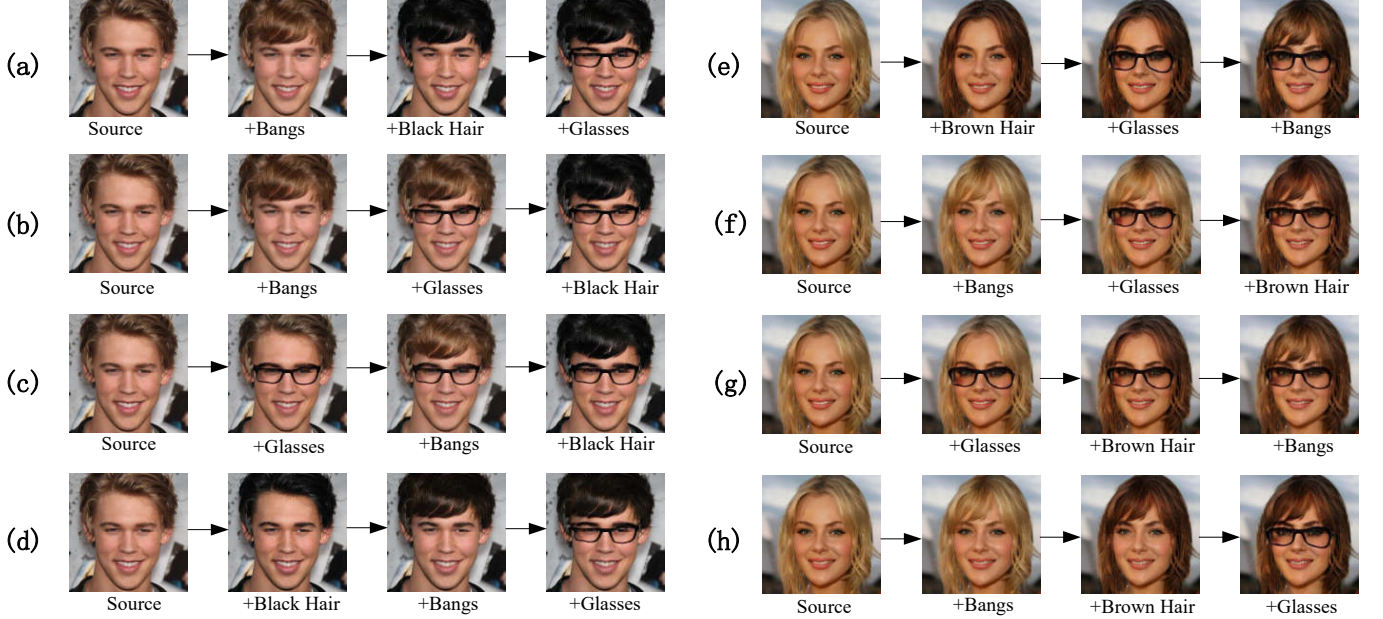


Fig. 8. The editing results of the editing continuity and consistency by CCR. The editing paths for (a) source \rightarrow +bangs \rightarrow +black hair \rightarrow +glasses; (b) source \rightarrow +bangs \rightarrow +glasses \rightarrow +black hair; (c) source \rightarrow +glasses \rightarrow +bangs \rightarrow +black hair; (d) source \rightarrow +black hair \rightarrow +bangs \rightarrow +glasses; (e) source \rightarrow +brown hair \rightarrow +glasses \rightarrow +bangs; (f) source \rightarrow +bangs \rightarrow +glasses \rightarrow +brown hair; (g) source \rightarrow +glasses \rightarrow +brown hair \rightarrow +bangs and (h) source \rightarrow +bangs \rightarrow +brown hair \rightarrow +glasses.

hair. The experimental results show that CCR fully considers editing continuity, i.e., users can re-edit an edited facial image while preserving facial identity and retaining all the previously edited attributes unchanged.

Editing consistency: The final editing results of AttGAN and STGAN have a larger margin when swapping attribute editing orders. The reason is that both methods are limited to editing continuity and can not be realized editing consistency. Although HiSD can retain the edited attributes, it has an inconsistent editing result when swapping attribute editing orders, e.g., swap the style codes of bangs and glasses. It is owing to that HiSD does not consider editing consistency. CCR can obtain a consistent and high-quality editing result in two different editing paths. The successful editing results are attributed to adversarial, reconstruction, and consistency loss in multi-domain. The experimental results show that CCR fully considers editing continuity and consistency. Users can generate high-quality editing results while retaining their desired attributes after sequential editing. CCR allows users to produce a consistent editing result despite swapping attribute editing orders.

We quantitatively analyze the results of two different editing

paths, as shown in Table II. For each method, the above path is denoted as Path 1, while the above path is denoted as Path 2. We can see that CCR has a higher editing accuracy on both editing paths than all the competing methods. Our method is better than peer methods in all the image quality evaluation metrics. STGAN has a lower editing accuracy than HiSD, while it has a better performance in image quality evaluation metrics. We visualize the editing results of STGAN and find that the output image is too smooth to retain its raw features, as shown in Fig. 7. The processing of pixels in STGAN makes a better performance in image quality evaluation metrics, while its editing accuracy is lower than HiSD. In Table II, the quantitative experimental results show that CCR performs well in both editing accuracy and image quality evaluation metrics. It is due to that CCR fully considers editing continuity and consistency. More editing results of editing continuity and consistency in Fig. 8 and extra evaluated results in Table III further demonstrate the well performance of CCR.

D. Reversibility

We further investigate the editing reversibility of CCR. We use RAC in Eq. 11 to evaluate the attribute remove accuracy

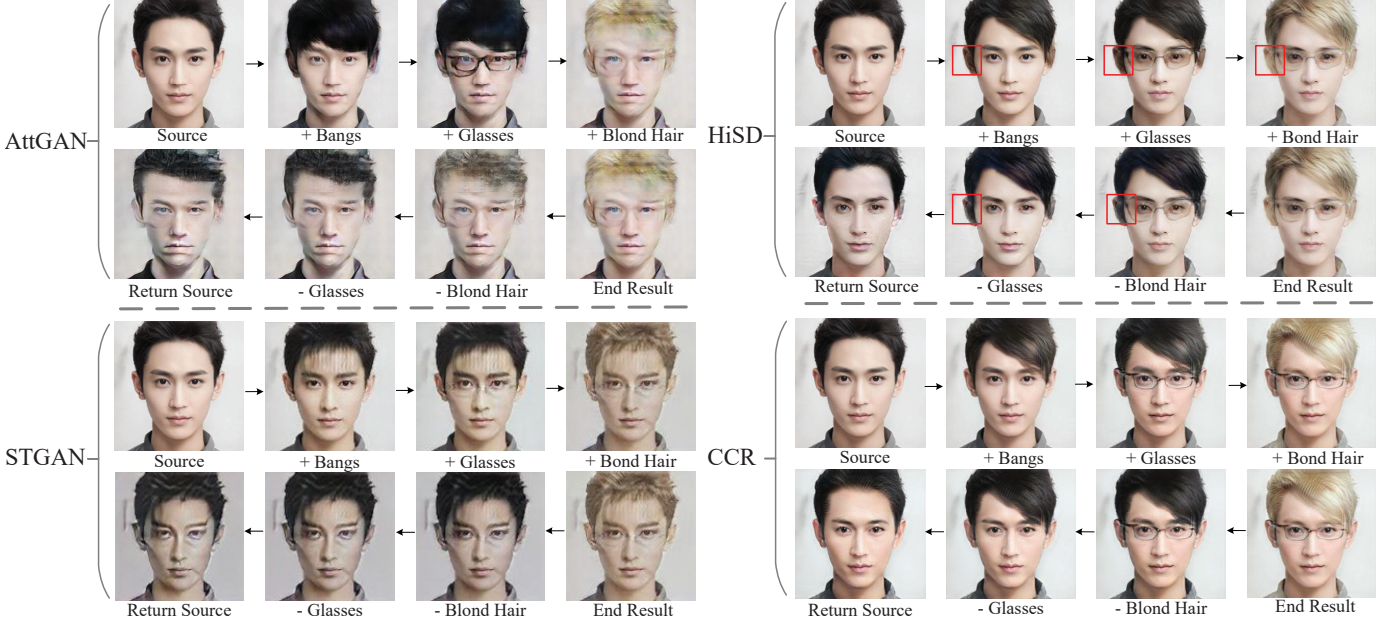


Fig. 9. The editing result of the editing reversibility compared to AttGAN [6], STGAN [7], HiSD [9]. Image artifacts are labeled with a red box in poorly edited images.

TABLE III

THE QUANTITATIVE RESULTS FOR COMPARING EDITING CONTINUITY AND CONSISTENCY ON ATTGAN [6], STGAN [7] HiSD [9] AND CCR BASED MORE IMAGE QUALITY METRICS.

Method	VSI \uparrow	VIF \uparrow	FSIM \uparrow	GMSD \uparrow	LPIPS \uparrow	DISTS \uparrow
AttGAN	0.9620	0.3815	0.8837	0.8684	0.8658	0.8825
STGAN	0.9624	0.3774	0.9037	0.8902	0.9340	0.8971
HiSD	0.9743	0.4857	0.9216	0.9071	0.9344	0.9246
CCR	0.9761	0.5554	0.9338	0.9177	0.9385	0.9251

of the reversed facial image. The image quality metrics are used to evaluate the similarity between the source image and reversed one. The qualitative experimental results are shown in Fig. 9. AttGAN and STGAN can not add corresponding attributes to a person. Both methods can not generate high-quality reversed facial images and preserve facial identity. The results indicate that their editing is irreversible. HiSD can not edit blond hair completely since it suffers from attribute entanglement. Besides, it produces an image artifact when editing bangs, as shown in the red box in Fig. 9. These image artifacts remain when editing a facial image along an inverse editing path, returning a low-quality facial image and losing facial identity. The results indicate that HiSD does not consider editing reversibility. CCR can restore a source facial image well and remove the edited attributes correctly. The reason for the phenomenon is that CCR fully considers editing reversibility and multi-domain image reconstruction. The experimental results demonstrate that CCR is reversible and can achieve the goal of editing reversibility in comparison to the competing methods. The quantitative experimental results are shown in Table IV. AttGAN and STGAN have a high RAC value. However, both methods do not add desired attributes to a person but return a facial image that is similar to the source one. HiSD has a higher RAC value than AttGAN and STGAN,

and it is superior to both methods on the image evaluation metrics. CCR outperforms the three competing methods in all the metrics. CCR can return a facial image that is closer to the source image than the three competing methods. It also can retain the quality of the reversed image and preserve facial identity. The quantitative experimental results show that CCR can well do facial image editing with reversibility. More reversible editing results in Fig. 10 and quantitative results in Table V show that CCR can achieve editing reversibility in comparison to peer works.

E. Ablation studies

The encoder is expected to extract different image features rather than to focus on reconstructing facial identity, i.e., the encoder should be a generalized one. For this purpose, we add the identity loss [54], [55] to encoder training process while leaving the rest of the training process unchanged, forcing CCR tends to reconstruct facial identity. The quantitative results of with/without identity loss on single attribute editing accuracy, multi-domain EAC, and RAC are shown in Table VI. All the accuracy declines when adding identity loss to train the encoder except RAC. The results indicate that identity loss makes the encoder focus on facial identity while neglecting other significant image information. The encoder trained with

TABLE IV
THE QUANTITATIVE RESULTS OF EVALUATING EDITING REVERSIBILITY USING RAC AND IMAGE QUALITY METRICS.

Method	RAC \uparrow	MSE \downarrow	RMSE \downarrow	UQI \uparrow	SSIM \uparrow	PSNR \uparrow	MS-SIM \uparrow
AttGAN [6]	86.60%	0.0940	0.2986	0.7132	0.5926	10.7178	0.6513
STGAN [7]	90.94%	0.0843	0.2869	0.6772	0.5638	10.9477	0.7307
HiSD [9]	94.48%	0.0271	0.1606	0.8424	0.7237	16.0690	0.8153
CCR	94.97%	0.0223	0.1464	0.8590	0.7379	16.8443	0.8366

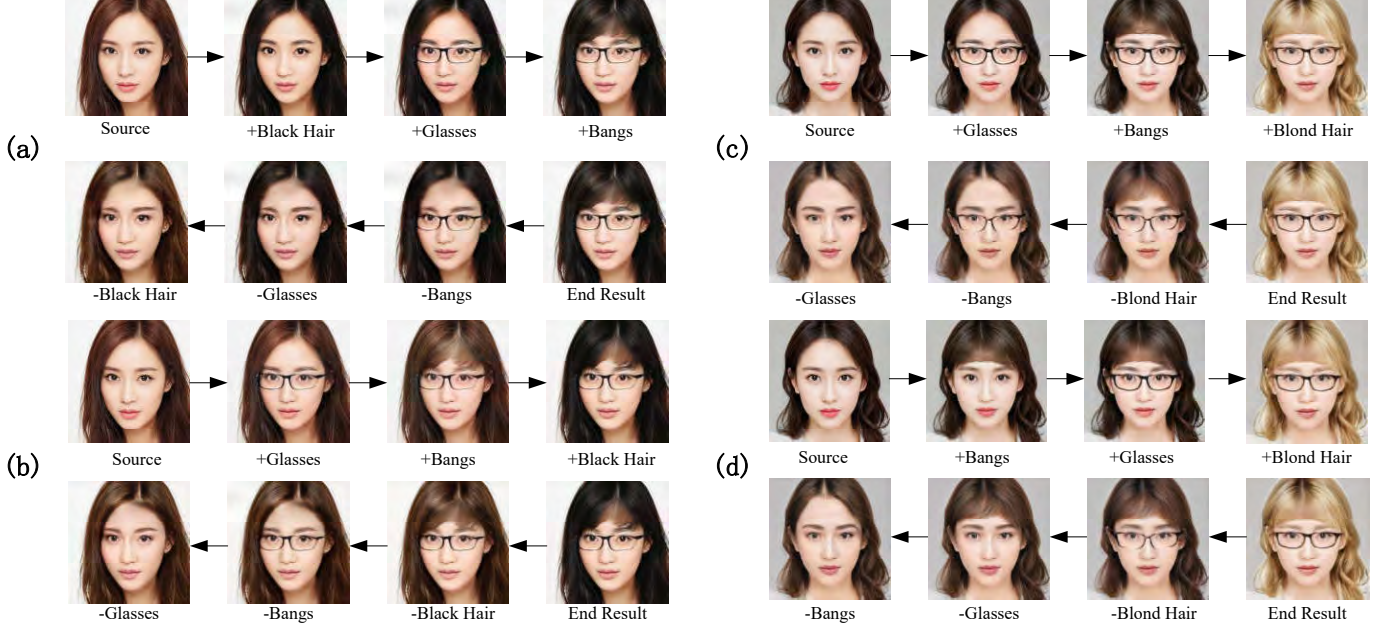


Fig. 10. The editing results of the editing reversibility by CCR. The editing paths for (a) source \rightarrow +black hair \rightarrow +glasses \rightarrow +bangs \rightarrow -bangs \rightarrow -glasses \rightarrow -black hair; (b) source \rightarrow +glasses \rightarrow +bangs \rightarrow +black hair \rightarrow -black hair \rightarrow -bangs \rightarrow -glasses; (c) source \rightarrow +glasses \rightarrow +bangs \rightarrow +blond hair \rightarrow -blond hair \rightarrow -bangs \rightarrow -glasses and (d) source \rightarrow +bangs \rightarrow +glasses \rightarrow +blond hair \rightarrow -blond hair \rightarrow -glasses \rightarrow -bangs.

TABLE V
THE QUANTITATIVE RESULTS FOR COMPARING EDITING REVERSIBILITY ON ATTGAN [6], STGAN [7] HiSD [9] AND CCR BASED MORE IMAGE QUALITY METRICS.

Method	VSI \uparrow	VIF \uparrow	FSIM \uparrow	GMSD \uparrow	LPIPS \uparrow	DISTS \uparrow
AttGAN	0.9249	0.1936	0.7782	0.8024	0.7235	0.7829
STGAN	0.9260	0.2316	0.8176	0.8362	0.8447	0.8100
HiSD	0.9473	0.2987	0.8450	0.8549	0.8368	0.8356
CCR	0.9488	0.3384	0.8564	0.86853	0.8387	0.8317

a specific loss can not extract global features and pass them to the next editing process, resulting in a sharp decline in editing accuracy. After investigating the training process of encoder, we experimentally conclude that the generalized encoder is a necessary condition to achieve the goal of editing continuity, consistency, and reversibility.

We config four feature fusion strategies to investigate attention and affine transformation modules. Fig. 11(a) is the experimental result after removing the attention and affine transformation module. From the fused feature map, we can see that some irrelevant regions are activated. It results in a large gap between the source image and generated one. In addition, the desired attribute is not edited to the facial image correctly. Fig. 11(b) presents the results that only retain the

affine transformation module. It can be seen that the regions unrelated to glasses in the fused feature map are not changed. The results indicate that CCR learns the disentangled style codes, which only contain attributes related to glasses and without affecting other attributes. Fig. 11(c) shows the results that only retain the attention module. The fused feature map shows that the regions related to glasses are activated while other regions remain unchanged. The glasses are edited to the generated facial image while other regions are obscured. Fig. 11(d) is the results that retain both modules. The fused feature map illustrates that the regions related to glasses are activated while other regions remain unchanged. We can get an edited facial image that wears glasses while hair color, bangs, and facial identity remain unchanged. We experimentally conclude

TABLE VI
THE QUANTITATIVE RESULTS OF WITH/WITHOUT IDENTITY LOSS ON SINGLE EAC, MULTI-DOMAIN EAC, AND RAC.

Method	EAC \uparrow		RAC \uparrow	Bangs	Black Hair	Blond Hair	Brown Hair	Glasses
	Path 1	Path 2						
Idloss [54]	54.90%	57.81%	95.63%	0.7418	0.8466	0.6859	0.5210	0.7231
No-Idloss	59.41%	60.49%	94.97%	0.9066	0.8935	0.8064	0.6100	0.9265

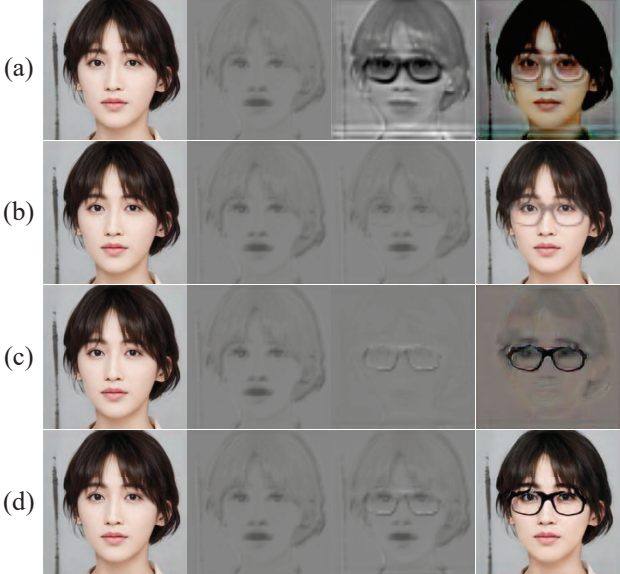


Fig. 11. The ablation studies for attention and affine transformation modules. Left to right for each line denotes: source image, feature map from encoder, fused feature map, and edited facial image.

that disentangled style codes and accurate attention regions are necessary condition for editing continuity, consistency, and reversibility.

IV. CONCLUSION AND DISCUSSION

In this work, we propose a novel method named CCR for facial image editing, which can achieve the goal of editing continuity, consistency, and reversibility. Extensive qualitative and quantitative experimental results demonstrate the effectiveness of the proposed method. Furthermore, we introduce a sufficient criterion, which can be used to determine whether a model is satisfied with continuity, consistency, and reversibility. We experimentally conclude that a generalized encoder, disentangled style codes, and accurate attention regions are the necessary conditions for editing continuity, consistency, and reversibility.

We take a first step towards a continuous, consistent, and reversible model. We believe that our proposed concepts and model will have promising prospects for multimedia applications, and we expect to create a graphical interface program, which can be integrated as a mobile application used in social software.

REFERENCES

[1] X. Chen, B. Ni, N. Liu, Z. Liu, Y. Jiang, L. Truong, and Q. Tian, “CooGAN: A Memory-Efficient Framework for High-Resolution Facial Attribute Editing,” in *Lecture Notes in Computer Science (including subseries Lecture Notes in Artificial Intelligence and Lecture Notes in Bioinformatics)*, vol. 12356 LNCS. Springer, 2020, pp. 670–686.

[2] K. Zhang, Y. Su, X. Guo, L. Qi, and Z. Zhao, “MU-GAN: Facial attribute editing based on multi-attention mechanism,” *IEEE/CAA J. Autom. Sin.*, 2020.

[3] Y. Liu, Q. Sun, X. He, A.-A. Liu, Y. Su, and T.-S. Chua, “Generating face images with attributes for free,” *IEEE Transactions on Neural Networks and Learning Systems*, vol. 32, no. 6, pp. 2733–2743, 2020.

[4] N. Yang, Z. Zheng, M. Zhou, X. Guo, L. Qi, and T. Wang, “A Domain-Guided Noise-Optimization-Based Inversion Method for Facial Image Manipulation,” *IEEE Transactions on Image Processing*, vol. 30, pp. 6198–6211, 2021.

[5] M. Shao, Y. Zhang, and Y. Fu, “Collaborative random faces-guided encoders for pose-invariant face representation learning,” *IEEE transactions on neural networks and learning systems*, vol. 29, no. 4, pp. 1019–1032, 2017.

[6] Z. He, W. Zuo, M. Kan, S. Shan, and X. Chen, “AttGAN: Facial Attribute Editing by only Changing What You Want,” *IEEE Transactions on Image Processing*, vol. 28, no. 11, pp. 5464–5478, 2019.

[7] M. Liu, Y. Ding, M. Xia, X. Liu, E. Ding, W. Zuo, and S. Wen, “STGAN: A unified selective transfer network for arbitrary image attribute editing,” *Proceedings of the IEEE Computer Society Conference on Computer Vision and Pattern Recognition*, vol. 2019-June, pp. 3668–3677, 2019.

[8] T. Xiao, J. Hong, and J. Ma, “ELEGANT: Exchanging latent encodings with GAN for transferring multiple face attributes,” in *Lecture Notes in Computer Science (including subseries Lecture Notes in Artificial Intelligence and Lecture Notes in Bioinformatics)*, vol. 11214 LNCS, 2018, pp. 172–187.

[9] X. Li, S. Zhang, J. Hu, L. Cao, X. Hong, X. Mao, F. Huang, Y. Wu, and R. Ji, “Image-to-image Translation via Hierarchical Style Disentanglement,” in *Proceedings of the IEEE Computer Society Conference on Computer Vision and Pattern Recognition*, 2021, pp. 8635–8644. [Online]. Available: <http://arxiv.org/abs/2103.01456>

[10] Y. Viazovetskyi, V. Ivashkin, and E. Kashin, “StyleGAN2 Distillation for Feed-Forward Image Manipulation,” in *Lecture Notes in Computer Science (including subseries Lecture Notes in Artificial Intelligence and Lecture Notes in Bioinformatics)*, vol. 12367 LNCS. Springer, 2020, pp. 170–186.

[11] G. Yang, N. Fei, M. Ding, G. Liu, Z. Lu, and T. Xiang, “L2M-GAN: Learning to Manipulate Latent Space Semantics for Facial Attribute Editing,” in *Proceedings of the IEEE Computer Society Conference on Computer Vision and Pattern Recognition*, 2021, pp. 2950–2959.

[12] N. Yang, M. Zhou, B. Xia, X. Guo, and L. Qi, “Inversion Based on a Detached Dual-Channel Domain Method for StyleGAN2 Embedding,” *IEEE Signal Processing Letters*, vol. 28, pp. 553–557, 2021.

[13] D. Liu, X. Gao, N. Wang, J. Li, and C. Peng, “Coupled attribute learning for heterogeneous face recognition,” *IEEE Transactions on Neural Networks and Learning Systems*, vol. 31, no. 11, pp. 4699–4712, 2020.

[14] M. Pang, B. Wang, M. Ye, Y.-m. Cheung, Y. Chen, and B. Wen, “DisP+ V: A Unified Framework for Disentangling Prototype and Variation From Single Sample per Person,” *IEEE Transactions on Neural Networks and Learning Systems*, 2021.

[15] R. Abdal, Y. Qin, and P. Wonka, “Image2StyleGAN++: How to edit the embedded images?” in *Proceedings of the IEEE Computer Society Conference on Computer Vision and Pattern Recognition*, 2020, pp. 8293–8302.

[16] T. Karras, S. Laine, M. Aittala, J. Hellsten, J. Lehtinen, and T. Aila, “Analyzing and improving the image quality of stylegan,” *Proceedings of the IEEE Computer Society Conference on Computer Vision and Pattern Recognition*, pp. 8107–8116, 2020.

[17] T. Karras, S. Laine, and T. Aila, “A style-based generator architecture for generative adversarial networks,” *Proceedings of the IEEE Computer*

Society Conference on Computer Vision and Pattern Recognition, vol. 2019-June, pp. 4396–4405, 2019.

[18] M. Pang, Y.-M. Cheung, Q. Shi, and M. Li, “Iterative dynamic generic learning for face recognition from a contaminated single-sample per person,” *IEEE Transactions on Neural Networks and Learning Systems*, vol. 32, no. 4, pp. 1560–1574, 2020.

[19] Y. Shen, C. Yang, X. Tang, and B. Zhou, “InterFaceGAN: Interpreting the Disentangled Face Representation Learned by GANs,” *IEEE Transactions on Pattern Analysis and Machine Intelligence*, 2020.

[20] Y. Shen and B. Zhou, “Closed-Form Factorization of Latent Semantics in GaNs,” in *Proceedings of the IEEE Computer Society Conference on Computer Vision and Pattern Recognition*, 2021, pp. 1532–1540.

[21] P. Upchurch, J. Gardner, G. Pleiss, R. Pless, N. Snavely, K. Bala, and K. Weinberger, “Deep feature interpolation for image content changes,” in *Proceedings - 30th IEEE Conference on Computer Vision and Pattern Recognition, CVPR 2017*, vol. 2017-January, 2017, pp. 6090–6099.

[22] A. Radford, L. Metz, and S. Chintala, “Unsupervised representation learning with deep convolutional generative adversarial networks,” *arXiv Prepr. arXiv1511.06434*, 2015.

[23] E. Richardson, Y. Alaluf, O. Patashnik, Y. Nitzan, Y. Azar, S. Shapiro, and D. Cohen-Or, “Encoding in Style: A StyleGAN Encoder for Image-to-Image Translation,” in *Proceedings of the IEEE Computer Society Conference on Computer Vision and Pattern Recognition*, 2021, pp. 2287–2296.

[24] J. Zhang, Y. Huang, Y. Li, W. Zhao, and L. Zhang, “Multi-Attribute transfer via disentangled representation,” in *33rd AAAI Conference on Artificial Intelligence, AAAI 2019, 31st Innovative Applications of Artificial Intelligence Conference, IAAI 2019 and the 9th AAAI Symposium on Educational Advances in Artificial Intelligence, EAAI 2019*, vol. 33, no. 01, 2019, pp. 9195–9202.

[25] F. Zhu, H. Cao, Z. Feng, Y. Zhang, W. Luo, H. Zhou, M. Song, and K. K. Ma, “Semi-supervised eye makeup transfer by swapping learned representation,” in *Proceedings - 2019 International Conference on Computer Vision Workshop, ICCVW 2019*, 2019, pp. 3858–3867.

[26] Y. L. Tong, *The multivariate normal distribution*. Springer Science & Business Media, 2012.

[27] T. Moore and M. Fallah, “Control of eye movements and spatial attention,” *Proceedings of the National Academy of Sciences of the United States of America*, vol. 98, no. 3, pp. 1273–1276, 2001.

[28] A. Pumarola, A. Agudo, A. M. Martinez, A. Sanfeliu, and F. Moreno-Noguer, “GANimation: Anatomically-aware facial animation from a single image,” in *Lecture Notes in Computer Science (including subseries Lecture Notes in Artificial Intelligence and Lecture Notes in Bioinformatics)*, vol. 11214 LNCS, 2018, pp. 835–851.

[29] K. De Bot, P. Gommans, and C. Rossing, “L1 loss in an L2 environment: Dutch immigrants in France,” *First Lang. attrition*, pp. 87–98, 1991.

[30] L. Mescheder, A. Geiger, and S. Nowozin, “Which training methods for GANs do actually converge?” in *35th International Conference on Machine Learning, ICML 2018*, vol. 8. PMLR, 2018, pp. 5589–5626.

[31] X. Wei, H. Shen, Y. Li, X. Tang, F. Wang, M. Kleinsteuber, and Y. L. Murphrey, “Reconstructible nonlinear dimensionality reduction via joint dictionary learning,” *IEEE transactions on neural networks and learning systems*, vol. 30, no. 1, pp. 175–189, 2018.

[32] Z. Li, Z. Zhang, J. Qin, Z. Zhang, and L. Shao, “Discriminative fisher embedding dictionary learning algorithm for object recognition,” *IEEE transactions on neural networks and learning systems*, vol. 31, no. 3, pp. 786–800, 2019.

[33] T. Miyato, T. Kataoka, M. Koyama, and Y. Yoshida, “Spectral normalization for generative adversarial networks,” *6th International Conference on Learning Representations, ICLR 2018 - Conference Track Proceedings*, 2018.

[34] B. Zhao, B. Chang, Z. Jie, and L. Sigal, “Modular generative adversarial networks,” in *Lecture Notes in Computer Science (including subseries Lecture Notes in Artificial Intelligence and Lecture Notes in Bioinformatics)*, vol. 11218 LNCS, 2018, pp. 157–173.

[35] X. Huang, M. Y. Liu, S. Belongie, and J. Kautz, “Multimodal Unsupervised Image-to-Image Translation,” in *Lecture Notes in Computer Science (including subseries Lecture Notes in Artificial Intelligence and Lecture Notes in Bioinformatics)*, vol. 11207 LNCS, 2018, pp. 179–196.

[36] Y. Wang, A. Gonzalez-Garcia, J. Van De Weijer, and L. Herranz, “SDIT: Scalable and diverse cross-domain image translation,” in *MM 2019 - Proceedings of the 27th ACM International Conference on Multimedia*, 2019, pp. 1267–1276.

[37] Y. Choi, M. Choi, M. Kim, J. W. Ha, S. Kim, and J. Choo, “StarGAN: Unified Generative Adversarial Networks for Multi-domain Image-to-Image Translation,” in *Proceedings of the IEEE Computer Society Conference on Computer Vision and Pattern Recognition*, 2018, pp. 8789–8797.

[38] M. Norouzi, D. J. Fleet, and R. Salakhutdinov, “Hamming distance metric learning,” in *Advances in Neural Information Processing Systems*, vol. 2, 2012, pp. 1061–1069.

[39] D. Guo, S. Shamai, and S. Verdú, “Mutual information and MMSE in Gaussian channels,” *IEEE International Symposium on Information Theory - Proceedings*, vol. 51, no. 4, p. 347, 2004.

[40] T. Chai and R. R. Draxler, “Root mean square error (RMSE) or mean absolute error (MAE)? -Arguments against avoiding RMSE in the literature,” *Geoscientific Model Development*, vol. 7, no. 3, pp. 1247–1250, 2014.

[41] A. Hore and D. Ziou, “Image quality metrics: PSNR vs. SSIM,” in *2010 20th Int. Conf. Pattern Recognit.*, 2010, pp. 2366–2369.

[42] Z. Wang and A. C. Bovik, “A universal image quality index,” *IEEE Signal Processing Letters*, vol. 9, no. 3, pp. 81–84, 2002.

[43] Z. Wang, A. C. Bovik, H. R. Sheikh, and E. P. Simoncelli, “Image quality assessment: From error visibility to structural similarity,” *IEEE Transactions on Image Processing*, vol. 13, no. 4, pp. 600–612, 2004.

[44] J. Snell, K. Ridgeway, R. Liao, B. D. Roads, M. C. Mozer, and R. S. Zemel, “Learning to generate images with perceptual similarity metrics,” in *2017 IEEE Int. Conf. Image Process.* IEEE, 2017, pp. 4277–4281.

[45] L. Zhang, Y. Shen, and H. Li, “VSI: A visual saliency-induced index for perceptual image quality assessment,” *IEEE Transactions on Image Processing*, vol. 23, no. 10, pp. 4270–4281, 2014.

[46] H. R. Sheikh and A. C. Bovik, “Image information and visual quality,” *IEEE Transactions on image processing*, vol. 15, no. 2, pp. 430–444, 2006.

[47] L. Zhang, L. Zhang, X. Mou, and D. Zhang, “FSIM: A feature similarity index for image quality assessment,” *IEEE transactions on Image Processing*, vol. 20, no. 8, pp. 2378–2386, 2011.

[48] W. Xue, L. Zhang, X. Mou, and A. C. Bovik, “Gradient magnitude similarity deviation: A highly efficient perceptual image quality index,” *IEEE transactions on image processing*, vol. 23, no. 2, pp. 684–695, 2013.

[49] R. Zhang, P. Isola, A. A. Efros, E. Shechtman, and O. Wang, “The unreasonable effectiveness of deep features as a perceptual metric,” in *Proceedings of the IEEE conference on computer vision and pattern recognition*, 2018, pp. 586–595.

[50] K. Ding, K. Ma, S. Wang, and E. P. Simoncelli, “Image quality assessment: Unifying structure and texture similarity,” *arXiv preprint arXiv:2004.07728*, 2020.

[51] T. Karras, T. Aila, S. Laine, and J. Lehtinen, “Progressive growing of gans for improved quality, stability, and variation,” *arXiv Prepr. arXiv1710.10196*, 2017.

[52] Z. Liu, P. Luo, X. Wang, and X. Tang, “Deep learning face attributes in the wild,” in *Proc. IEEE Int. Conf. Comput. Vis.*, vol. 2015 International Conference on Computer Vision, ICCV 2015, 2015, pp. 3730–3738.

[53] A. Paszke, S. Gross, S. Chintala, G. Chanan, E. Yang, and ..., “Automatic differentiation in pytorch,” 2017. [Online]. Available: <https://openreview.net/forum?id=BJJsrmfCZ>

[54] J. Deng, J. Guo, N. Xue, and S. Zafeiriou, “ArcFace: Additive angular margin loss for deep face recognition,” in *Proceedings of the IEEE Computer Society Conference on Computer Vision and Pattern Recognition*, vol. 2019-June, 2019, pp. 4685–4694.

[55] D. S. Tan, J. H. Soeseno, and K. L. Hua, “Controllable and Identity-Aware Facial Attribute Transformation,” *IEEE Transactions on Cybernetics*, 2021.